SCIENTIFIC JOURNAL
EARTH'S CRYOSPHERE

Kriosfera Zemli, 2015, vol. XIX, No. 1, pp. 20–26 **http://www.izdatgeo.ru**

PHYSICOCHEMICAL PROCESSES IN ICE AND PERMAFROST

WATER VAPOR FLOWS ACROSS SNOW–AIR AND SNOW–SOIL INTERFACES

V.N. Golubev, D.M. Frolov

Lomonosov Moscow State University, Laboratory of Snow Avalanches and Mudflows, Department of Geography, 1 Leninskie Gory, Moscow, 119991, Russia; golubev@geol.msu.ru

Gradients of water vapor concentration in snow are due to the presence of temperature gradients. Vapor concentration gradients exist also at the snow–air and snow–soil interfaces because the content of pore vapor in snow differs from those in air and soil immediately above and below it, respectively. The gradients drive sublimation of ice and transport of the forming vapor. Sublimation of snow at constant temperature depends on its thermal conductivity and density controlled by microstructure and varies from $42 \cdot 10^{-8}$ kg/(m^2·s) at –8 °C for ice and $40 \cdot 10^{-8}$ kg/(m^2·s) for snow with 500 kg/m^3 density to $32 \cdot 10^{-8}$ kg/(m^2·s) for 160 kg/m^3 snow. The concentration of vapor in the pore space of snow, relative to the theoretical value defined by the Clausius–Clapeyron equation, is 1.08 at –22 °C and 1.045 at –5 °C. Vapor flows across the snow-soil interface are in the ranges $(8.0–39.3) \cdot 10^{-8}$ kg/(m^2·s), from soil to snow, and $(1.0–2.5) \cdot 10^{-8}$ kg/(m^2·s), from snow to soil, as estimated for sand and clay models in the absence and in the presence of temperature gradient.

Mass transfer, snow, sublimation, water vapor

INTRODUCTION

Both perennial and seasonal snow has uneven temperature patterns, and its pore space stores variable concentrations of water vapor. The gradients of temperature and vapor concentration in snow lying between air and soil are due mainly to its thermal state which controls the respective flows of mass and heat [*Pavlov, 1975; Golubev and Ermakov, 1993*]. Additional variations of vapor concentration at the snow–air and snow–soil interfaces arise because the amount of pore vapor in snow differs from that in air and soil immediately above and below the snow cover.

Ice crystals form in the atmosphere supersaturated with water vapor. Having precipitated on the surface, they commonly get into undersaturated conditions, while the falling and depositing snow flakes undergo sublimation [*Callaghan et al., 2011*]. Sublimated snow makes about 10 % of solid precipitation in the snow budget over most of the Russian territory, and is locally up to 30 % [*Pavlov, 1975*]. The total share of sublimation may reach 50 % relative to the total amount of frozen precipitation and up to 35 % of annual precipitation in the Arctic moisture budget [*Box and Steffen, 2001; Liston and Sturm, 2004; Strasser et al., 2008; Neumann et al., 2009*].

The direction and rate of vapor flow across the snow–soil interface depend on the respective gradients of temperature and pore moisture concentration [*Pavlov, 1975; Golubev and Guseva, 1987; Golubev et al., 1997*].

PROBLEM FORMULATION

In steady air conditions, snow sublimation is interpreted as water vapor transport from the snow surface through the boundary layer of air of the thickness h_a, where vapor concentration undergoes most of change (Fig. 1). In this case, the sublimation i can be described by Fick's diffusion equation [*Golubev and Guseva, 1987; Golubev et al., 1997*]:

$$i = D \operatorname{grad} C,$$

where D is the vapor diffusion in air; $\operatorname{grad} C = \Delta C/h = (C_s - C_a)/h_a$, $\Delta C = C_s - C_a$ is the vapor concentration difference between snow surface C_s and air C_a. Vapor concentration and temperature mostly change within the zones h_a and h_{sn} in the immediate vicinity of the interfaces. The concentration of vapor in the atmosphere depends on air temperature and relative humidity. Near the interfaces, it is commonly assumed to correspond to the surface temperature T_s, while the thickness of the transition layer can be inferred from vapor diffusion and thermal diffusivity of air [*Kutateladze and Borshanskiy, 1958; Mikheev and Mikheeva, 1977*]. The transition layer has a stable stratification with denser air at the bottom [*Kutateladze and Borshanskiy, 1958*].

When modeling sublimation, the temperatures of air (T_a) and snow (T_{sn}) are assumed to be equal at the interface, and air is assumed to be saturated with respect to water vapor. The thermal interaction at the interface occurs as [*Kutateladze and Borshanskiy, 1958; Mikheev and Mikheeva, 1977*]

$$T_a = T_{sn},\ \lambda_{sn}\left(\frac{\partial T_{sn}}{\partial Z}\right) = L_{iv} i - \lambda_a \left(\frac{\partial T_a}{\partial Z}\right), \qquad (1)$$

where T_{sn} and T_a, λ_{sn} and λ_a are, respectively, the temperatures and thermal conductivities of snow and humid air; $\partial T_a/\partial Z$ and $\partial T_{sn}/\partial Z$ are the interface temperature gradients; L_{iv} is the sublimation heat; i is the sublimation; Z is the vertical coordinate.

Equation (1) can be transformed to

$$i = \frac{1}{L_{iv}}\left[\lambda_{sn}\left(\frac{\partial T_{sn}}{\partial Z}\right) + \lambda_a \left(\frac{\partial T_a}{\partial Z}\right)\right]. \qquad (2)$$

Temperature gradients in snow and air depend on thermal conductivity and sublimation rate. The thermal conductivity of snow depends much more strongly on density than on temperature [*Sturm et al., 1997*]. The temperature dependence of air thermal conductivity is as small as ~10^{-3} %/K, i.e., λ_a is almost invariable at normal temperature patterns. The thermal conductivity of air is at least ten times less than that of snow [*Pavlov, 1975; Mikheev and Mikheeva, 1977*]: $\lambda_a = \eta\lambda_{sn}$, $\eta \ll 1$. Substituting this into (2) and differentiating with respect to snow thermal conductivity (λ_{sn}) lead to the respective derivative of sublimation defined by the interface temperature gradient:

$$\frac{\partial}{\partial \lambda} i = \frac{1}{L_{iv}}\left[\left(\frac{\partial T_{sn}}{\partial Z}\right) + \eta\left(\frac{\partial T_{sn}}{\partial Z}\right)\right]. \qquad (3)$$

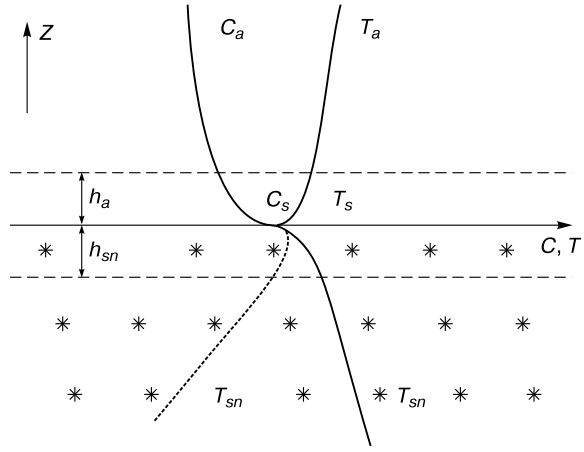

Fig. 1. Patterns of air (T_a), snow (T_{sn}), and snow surface T_s temperatures and water vapor concentrations in air (C_a) and on snow surface (C_s).

Dash line shows another version of snow temperature variations $\left(T^*_{sn}\right)$ below the interface.

Most of the known λ_{sn} vs. ρ_{sn} regression equations (Table 1) are power functions: $\lambda_{sn} = k\rho_{sn}^n$, where k varies in a large range and the exponent n is from 1 to 4 [*Pavlov, 1975; Golubev and Guseva, 1987; Sturm et al., 1997*]. The snow sublimation derivative with

Table 1. **Effective thermal conductivity λ_s vs. snow density ρ_s and temperature [*Pavlov, 1975; Sturm et al., 1997 and references therein*]**

Reference	Thermal conductivity regression equation λ_s [W/(m·K)] vs. ρ_s [kg/m^3]	Density, kg/m^3	Negative temperatures, °C
Yosida and Iwai, 1950	$\lg \lambda_s = (2\cdot10^{-3})\rho_s - 1.378$	72–400	1–6
Dyachkova and Serova, 1960	$\lg \lambda_s = (2.25\cdot10^{-3})\rho_s - 1.42$	80–470	–
Izumi and Fujioka, 1967	$\lg \lambda_s = (2.16\cdot10^{-3})\rho_s - 1.17$	80–500	–
Lzumi and Huzioka, 1975	$\lg \lambda_s = (2.16\cdot10^{-3})\rho_s - 1.11$; $\lg \lambda_s = (1.7\cdot10^{-3})\rho_s - 1.2$	73–483	–
Sakazume and Seki, 1980	$\lg \lambda_s = -1.25 + (2.12\cdot10^{-3})\rho_s$	150–700	0–16
Lange, 1985	$\lg \lambda_s = -3 + (6.9\cdot10^{-3})\rho_s$	230–420	4–20
Sulakvelidze, 1955	$\lambda_s = (0.5107\cdot10^{-3})\rho_s$	<350	2–13
Proskuryakov, 1957	$\lambda_s = 0.02093 + (1.01\cdot10^{-3})\rho_s$	140–310	–
Abel's, 1892	$\lambda_s = (2.846\cdot10^{-6})\rho_s^2$	140–330	10–30
Devaux, 1933	$\lambda_s = 0.0293 + (2.93\cdot10^{-6})\rho_s^2$	90–590	5–20
Kondrat'eva, 1945	$\lambda_s = (3.558\cdot10^{-6})\rho_s^2$	330–500	2–13
Bracht, 1949	$\lambda_s = (2.051\cdot10^{-6})\rho_s^2$	90–635	3–13.5
Yen, 1965	$\lambda_s = (3.223\cdot10^{-6})\rho_s^2$	400–590	6–11
Murakami and Maeno, 1989	$\lambda_s = 0.102 - (1.04\cdot10^{-3})\rho_s + (3.73\cdot10^{-6})\rho_s^2$	246–917	11
Ostin and Andersson, 1991	$\lambda_s = -0.00871 + (4.39\cdot10^{-4})\rho_s + (1.05\cdot10^{-6})\rho_s^2$	77–684	6.5–19.9
Sturm et al., 1997	$\lambda_s = 0.138 - (1.01\cdot10^{-3})\rho_s + (3.233\cdot10^{-6})\rho_s^2$	156–600	–
VanDusen, 1929	$\lambda_s = 0.021 + (0.42\cdot10^{-3})\rho_s + (2.16\cdot10^{-9})\rho_s^3$	–	–
Pavlov, 1973	$\lambda_s = 3.49\cdot10^{-3} + (3.52\cdot10^{-4})\rho_s - (2.06\cdot10^{-7})\rho_s^2 + (2.62\cdot10^{-9})\rho_s^3$	120–350	1–25
Jannson, 1901	$\lambda_s = 0.02093 + (0.7953\cdot10^{-3})\rho_s + (2.512\cdot10^{-12})\rho_s^4$	47–470	1–13

respect to thermal conductivity can be presented as the linear density dependence

$$\frac{\partial}{\partial \rho_{sn}} i = \frac{1}{L_{iv}} \left[\left(\frac{\partial T_{sn}}{\partial Z} \right) + \eta \left(\frac{\partial T_a}{\partial Z} \right) \right] 2k\rho_{sn}. \qquad (4)$$

EXPERIMENTAL METHODS

Sublimation and mass transfer measurements in samples of snow, ice, and frozen soil were carried out in a thermally insulated box (0.7 m long, 0.65 m wide, and 0.5 m high), where a certain thermal regime was maintained. Sublimation was studied at –4, –8 and –18 °C, with a total duration of experimental runs 1600 hr. The samples, with their densities 917 kg/m^3 (ice), 500, 330, and 160 kg/m^3 (snow) and 1560 kg/m^3 (frozen soil), were placed in cylindrical capsules of foamed polyurethane, 0.08 m in diameter and 0.05 m high.

Temperature and humidity in the box were measured by *Tinytag Ultra 2* loggers (to an accuracy no worse than 0.7 °C and 3 %, the designed instrument resolution being at least 0.01 °C and 0.3 %, respectively). Temperatures inside and above the samples were taken with T-type copper-constantan thermocouples and recorded by the *Agilent 34970A* data acquisition unit with a resolution no lower than 0.001 °C. The correction applied to readings of each thermocouple did not exceed 0.5 °C, according to preliminary calibration.

DISCUSSION

Sublimation of snow, ice, and frozen soil. According to (1)–(4), sublimation depends on thermal conductivity and temperature gradients across interfaces. The density dependence of snow thermal conductivity means that the denser the snow the faster its sublimation, with the maximum for ice. This inference has been supported by sublimation experiments with frozen soil, ice, and snow samples of different densities for 1600 hr in quasi-stationary conditions, at –8 °C in the absence of wind (Fig. 2). In the presence of wind, the relationship is only valid for sublimation of firn and ice that almost lack open pores and have the density at least 630 kg/m^3.

As follows from the Clausius–Clapeyron equation, the concentration of water vapor in pores and voids of snow (C_{sn}) corresponds to that of saturated vapor over the ice surface C_i, given by

$$C_i(T) = C_0 \exp\left[\frac{L_{iv}}{R} \left(\frac{T - T_0}{TT_0} \right) \right], \qquad (5)$$

where C_0 is the concentration of saturated vapor at T_0 = 273.15 K; L_{iv} is the ice sublimation heat; R is the gas constant.

Snow sublimation in a thermally insulated box at an average temperature of –8 °C led to a pattern (Fig. 3) with low temperatures to 20 cm above the interface in air and to 10 cm below it in snow, the coldest (–8.9 °C) at the interface and within 1 cm snow depth.

The interface temperature can be presented as [*Kutateladze and Borshanskiy, 1958*]

$$T_a - T_s = L_{iv}(\beta/\alpha)(e_n - e_a) \text{ at } \alpha/\beta = \rho_a c_a R_a T_a, \quad (6)$$

where T_s is the sublimation surface temperature; T_a is the air temperature at some distance to the surface; L_{iv} is the ice sublimation heat; e_s, e_a are the vapor partial pressures near the ice surface and in air, respectively; β, α are the coefficients of mass and heat transfer; c_a is the specific heat of humid air; R_a is the specific gas constant of humid air; ρ_a is the density of humid air. The vapor concentration in air (C_a) depends on its temperature and relative humidity, and the interface concentration C_s corresponds to saturation at the interface temperature T_s.

The vapor concentrations in the snow pore space and above the snow and ice surfaces measured in ex-

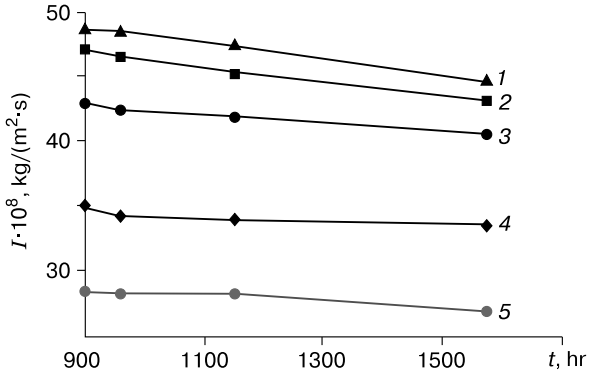

Fig. 2. Time-dependent (t) sublimation (I) of ice (*1*), frozen soil (*5*), and snow (*2–4*) of different densities: 500 kg/m^3 (*2*), 330 kg/m^3 (*3*), and 160 kg/m^3 (*4*).

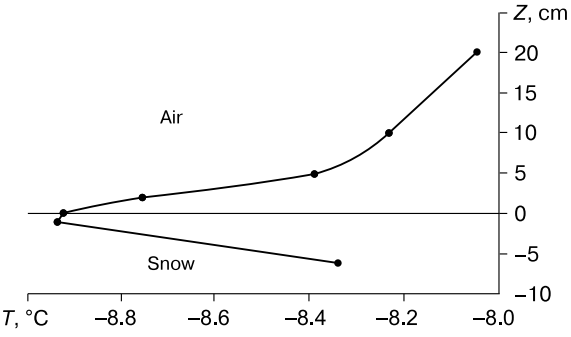

Fig. 3. Quasi-isothermal vertical temperature patterns in air and in 300 kg/m^3 snow.

Distance to interface (Z): 20, 10, 5, and 2 cm (above snow surface); 0 (on snow surface); 6 and 1 cm (below snow surface).

periments at –20 to –2.8 °C turned out to differ from the estimates predicted by (5) and those based on the total energy of H_2O escape from the ice structure according to the Clausius–Clapeyron equation (Fig. 4). The ratio of measured vapor concentrations in the snow pore space to the theoretical saturation above ice (C_{sn}/C_i) varied from 1.04 at –3 °C, to 1.06 at –12 °C, and to 1.08 at –22 °C. Elevated vapor concentrations were observed 1.5 cm above the snow surface (from absorption of λ = 6.3 μm IR radiation) and formed for 60–80 hours in a 10^{-3} m^3 isolated snow pore [*Golubev and Ermakov, 1993*]. Absolute supersaturation remained almost invariable upon cooling but its relative value increased rapidly, which may be responsible for the excess of sublimation over the theoretical predictions by (5) or (6).

The Thomson equation relating the equilibrium vapor pressure over a drop to its size can be converted to the case of solids; then it implies a higher share of vapor pressure over edges and vertices in the total value P_r over a crystal of the linear size r [*Golubev and Guseva, 1987*]. According to this equation, the magnitude of supersaturation depends on the size and geometry of crystals:

$$C(T,r) = C(T)\left(1 + F/r\right),$$

where $C(T, r)$ is the vapor concentration over grains with the average curvature radius r at the temperature T; $C(T)$ is the vapor concentration over a flat ice surface at the temperature T by the Clausius–Clapeyron equation. The crystal geometry parameter F refers to changes of the surface energy caused by changing relations among its faces (e.g., on transition from crystal growth to evaporation) and increases from $2{\cdot}10^{-5}$ m at equilibrium crystal geometry to $8{\cdot}10^{-5}$ m at a greater number of edges and vertices (deep hoar, snow flakes, etc.).

Mass transport across the snow-frozen ground interface. Intense capillary condensation of water vapor in soil begins at 0.80–0.85 relative humidity of the pore space [*Golubev and Ermakov, 1993*], i.e., relative content of pore water in undersaturated soil is commonly under this value. Soil moisture mainly exists as meniscus water at grain boundaries exposed to additional pressure controlled by the meniscus shapes, which are concave in moderately wet soil (Fig. 5). According to the Laplace equation, this corresponds to vapor pressure in soil pores lower for the value Δe:

$$\Delta e = -\left(\rho_v/\rho_w\right)\sigma\left(1/r_1 + 1/r_2\right),$$

where σ is the water surface tension; r_1, r_2 are the curvature radiuses of the meniscus surface; ρ_v/ρ_w is the vapor-to-water density ratio.

Changes in wetting of solid soil particles and soil moisture lead to the respective changes of meniscus curvature and vapor concentration. Specifically, the average meniscus curvature radius in medium-grained quartz sand is about 10^{-5} m and varies from $4{\cdot}10^{-5}$ m to $0.6{\cdot}10^{-5}$ m at water contents 20 % and 2 %, respectively.

In frozen soil, ice remains mainly confined to grain boundaries while the pore vapor concentration increases as the Laplace component disappears. The vapor concentration in a $1.5{\cdot}10^{-3}$ m^3 pore in frozen silt is 90 % at 5 % ice content but approaches saturation as the ice content increases to 30 %. However, the pore space of this undersaturated soil stores less vapor than snow pores, at the same temperature [*Golubev and Ermakov, 1993; Golubev et al., 1997*], which induces vapor flow from snow to soil.

In natural conditions, at normal soil-snow thermal relations, when soil is warmer than snow, vapor migrates from soil to the colder snow. However, the conditions of low temperature gradients across the soil-snow interface maintain dynamic equilibrium,

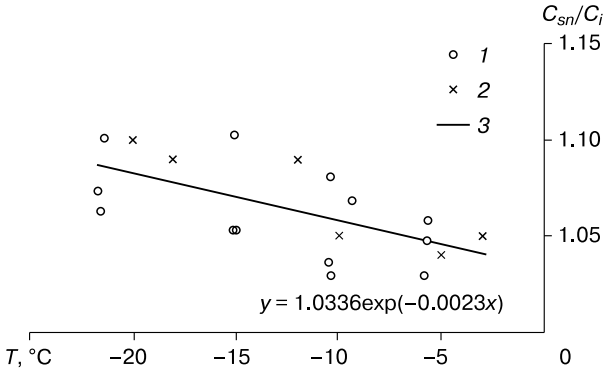

Fig. 4. Temperature dependence of relative water vapor concentration in snow pore space C_{sn}/C_i.

1, 2: C_{sn} measured with a *Tinytag Ultra 2* logger (1) and a hygrometer (*2*); *3*: trend.

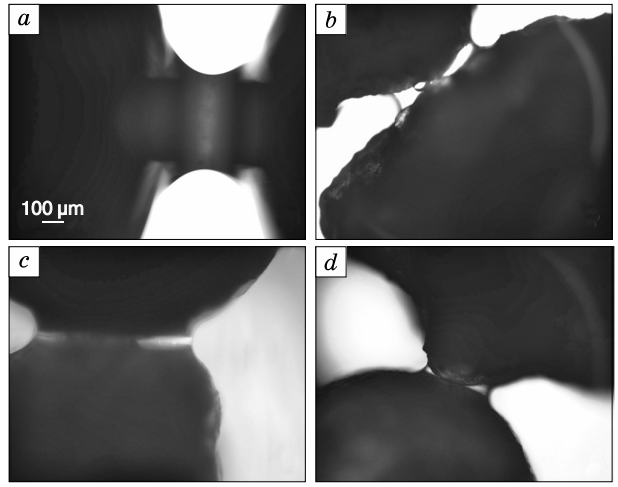

Fig. 5. Meniscus water at grain boundaries: locations and shapes.

Spherical particles (r = 1 mm), in model soil *(a)* and in real soil (*b–d*).

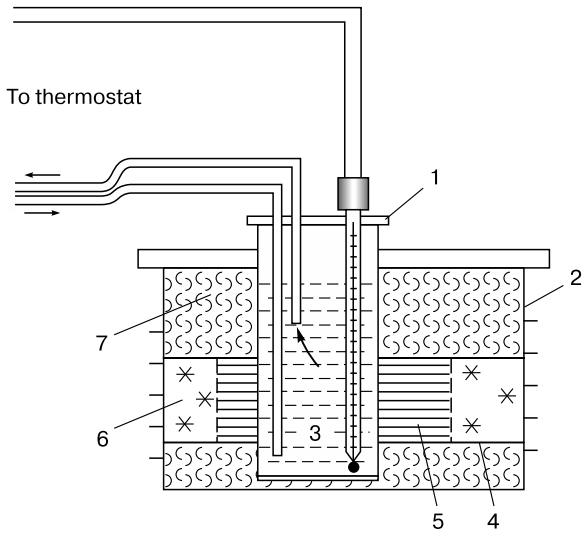

Fig. 6. Experiment for studying temperature gradient dependence of water vapor flow across the sample-air interface.

1 – container with thermostatic fluid; 2 – box; 3 – temperature controller; 4 – tubes with samples; 5 – soil or ice; 6 – snow; 7 – thermal insulator.

without preferred vapor flow direction. Moreover, vapor can also flow back from snow, where vapor concentration is higher than in soil.

Such a flow across the interface can be described by an equation similar to Fick's law

$$F_{\Delta C} = D_{g/s} \operatorname{grad} C_{g/s}, \qquad (7)$$

where $F_{\Delta C}$ is the flow due to vapor concentration difference between soil and snow; C is vapor concentration; the subscripts g and s refer to soil (ground) and snow, respectively; $D_{g/s}$ is the coefficient of mass transfer across the soil-snow interface; grad $C_{g/s} = (C_s - C_g)/\Delta x$ is the vapor concentration gradient; $\Delta x = \Delta x_s + \Delta x_g$ is the snow and soil depths to which most of vapor concentration changes are confined. $D_{g/s}$ in (7) depends on mass transfer coefficients in snow (Δx_s) and soil (Δx_g), respectively: $D_s = D_0(1 - \rho_s/\rho_i)$ and $D_g = D_0(1 - \rho_g/\rho_{mc})$, where D_0 is the vapor diffusion in air at the given temperature, and ρ_s, ρ_i, ρ_g, ρ_{mc} are, respectively, the densities of snow, ice, soil, and soil skeleton (matrix).

Mass transport driven by temperature gradient was studied experimentally using a box filled with a thermal insulator and a container connected to a thermostat placed in its center (Fig. 6), with –2 °C heating fluid circulating in the container-thermostat system; the temparture outside the box was maintained constant at –13.0 ± 0.5 °C. The samples of snow, ice, and frozen soil were placed in polyvinyl tubes, 8 cm in diameter. Two or three tubes of different lengths were assembled in a single column which was laid horizontally in the box with its two ends contacting the "warm" container and the "cold" metal box wall, respectively. This produced a temperature gradient and, correspondingly, a gradient of vapor concentration that drove horizontal mass transport from the warm end to the cold one. The sides of the samples were thermally insulated. The "warm" tubes were filled with ice or soil (sand, clay) which simulated the ground while the "cold" tubes contained snow. The temperatures of snow, ice, and soil at certain points in the tubes, were measrued daily, including 1 cm away from the surface. Mass flows were estimated by weighing each tube before and after the experiment.

The temperature gradient was calculated from the sample length and the temperature on the contact surfaces. In the absence of temperature gradient, a steady, though quite weak vapor flow from snow to soil formed across the interface between snow and frozen soil of different ice contents (9 to 100 %), as it was reported previously [*Golubev et al., 1997*] (Table 2).

Table 2. **Mass transfer across snow-soil (ice) interface with and without temperature gradient [*Golubev et al., 1997*]**

Interfaces	Temperature gradient, K/m	Interface temperature, °C	Vapor flow*, 10^{-8} kg/(m^2·s)	Concentration gradient, 10^{-3} kg/m^4
Snow/ice	0	–13.0	–0.516	0.392
Snow/sand, ice content 34 %	0	–13.0	–2.587	1.964
Snow/sand, ice content 100 %	0	–13.0	–1.020	0.770
Snow/sand, ice content 9 %	0	–4.0	–1.199	0.865
Snow/clay (kaolinite), ice content 15 %	0	–4.0	–1.279	0.923
Snow/sand, ice content 21 %	86	–5.0	39.3	19.45
Snow/sand, ice content 21 %	91	–7.0	28.1	14.07
Snow/clay silt, ice content 35 %	24	–8.3	8.1	4.05
Snow/clay silt, ice content 35 %	47	–5.3	12.8	6.42

* Positive and negative values correspond, respectively, to flows from soil to snow and back from snow to soil.

Estimates of isothermal (grad $T = 0$) snow-to-soil vapor flow were used to estimate vapor concentration gradients grad C across the interface using equation (6). In the absence of temperature gradient, the gradients of vapor concentration were $(0.39–1.96)\cdot10^{-2}$ kg/m^4, while the snow-to-soil vapor flow was $(0.5–2.6)\cdot10^{-8}$ kg/(m^2·s). At the gradients of temperature from 24 to 91 K/m, those of vapor concentration became more than ten times higher reaching $(5.07–19.45)\cdot10^{-2}$ kg/m^4, and the soil-to-snow flow reached $(8–40)\cdot10^{-8}$ kg/(m^2·s). This almost tenfold difference in vapor flows between the cases of absent and present temperature gradient implies that the direction of mass transport can change within a narrow range of thermal conditions at the snow-soil interface.

The flow direction depends on the predominant mass transfer component: either it is the flow driven by difference in pore vapor concentrations in thermally balanced snow and soil ($F_{\Delta C}$) or that induced by the temperature gradient in the snow-soil system ($F_{\Delta T}$). The critical temperature gradients, at which the flows $F_{\Delta T}$ and $F_{\Delta C}$ become equal, depend on the interface temperature and can be estimated from isothermal mass transport data (Table 2).

See the results of calculations for sand with different ice contents in Fig. 7: curves A and B correspond, respectively, to sand with ice contents 100 % and 34 %; the zones below and above the line A (B) represent, respectively, flows from snow to soil and from soil to snow. The vapor flow contour lines $(10, 30)\cdot10^{-8}$ kg/(m^2·s) characterize the combinations of temperatures and temperature gradients.

The vapor flows were studied experimentally with and without temperature gradient (Table 2). The data for isothermal conditions were plotted on the temperature axis at zero temperature gradient. The direction of vapor flow (from snow to soil or back) can change within a broad range of interface temperatures but in a relatively narrow range of temperature gradients across the snow-soil interface, which however often occurs in nature. The measured vapor flow from sand and clay silt with ice contents 21 % and 35 %, respectively, at relatively high temperature gradients, turned out to be lower than the theoretical value. The mismatch may be due to the presence of dry soil immediately at the snow boundary which reduces the concentration gradient of vapor and causes its flow from soil.

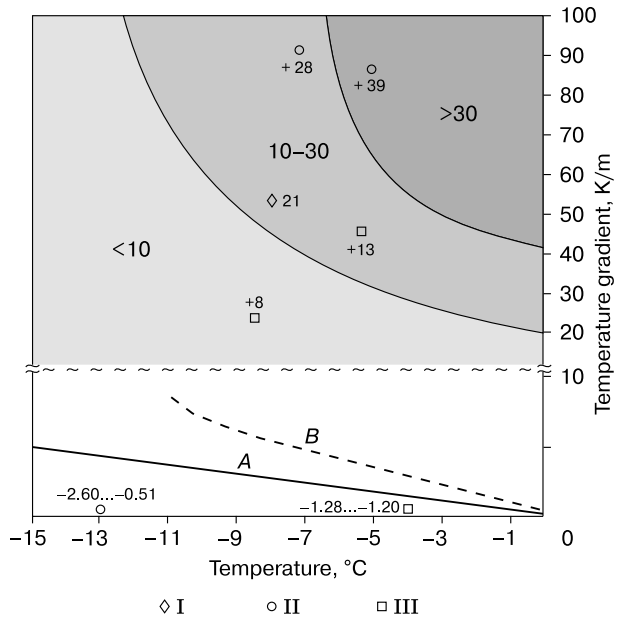

Fig. 7. Rate and direction of water vapor flow across the interface of snow with ice (I), frozen sand (II), or kaoline clay (III), as a function of temperature and temperature gradient.

Numerals near data points are flow rates in 10^{-8} kg/(m^2·s). Positive and negative values correspond, respectively, to soil-to-snow and snow-to-soil flow directions. Gray shades show zones of vapor flow from soil to snow at different rates: less than 10, 10–30, and more than 30 [10^{-8} kg/(m^2·s)]. Curves A and B correspond, respectively, to 100 % and 34 % ice contents in soil. Flow is from frozen sand above lines A (or B) or from snow to soil below lines A (or B).

CONCLUSIONS

Sublimation of –8 °C snow increases with its density from $32\cdot10^{-8}$ kg/(m^2·s) at 160 kg/m^3 to $40\cdot10^{-8}$ kg/(m^2·s) at 500 kg/m^3; in the case of ice, sublimation reaches $42\cdot10^{-8}$ kg/(m^2·s) but decreases to $26\cdot10^{-8}$ kg/(m^2·s) at the interface of ice with wet frozen sand.

Snow pores are supersaturated with water vapor (from 1.04 at –3 °C to 1.08 at –22 °C), due to surface energy of ice grains and high vapor concentrations over their edges, faces, and vertices.

The rate and direction of mass transport across the snow-soil interface depend on temperature, temperature gradient, ice content, and grain size of the soil. In the case of 100 % ice content, flow variations are controlled mainly by the morphology of snow grains (microstructure) but are almost independent of lithology. During vapor transport from snow to soil, evaporation is from the surface of cold snow grains while vapor becomes condensed upon relatively warmer soil particles with additional release of phase change heat. Thus, a counter heat flow arises against the general flow direction, which is consistent with the Le Châtelier–Brown principle.

Flow of vapor to soil and increase in its ice content or flow from soil and its drying are of limited spread and cause only weak influence on the total soil moisture budget. However, this factor is important in snow re-crystallization which may reduce its mechanic strength and cause snow instability on slopes.

References

Box, J.E., Steffen, K., 2001. Sublimation on the Greenland ice sheet from automated weather station observations. J. Geophys. Res. 106 (D24), 33,965–33,981.

Callaghan, T.V., Johansson, M., Brown, R.D., et al., 2011. The changing face of Arctic snow cover: A synthesis of observed and projected changes. AMBIO 40, 17–31.

Golubev, V.N., Guseva, E.V., 1987. Heat and mass transfer in stratified snow cover, in: Mountain Snow and Avalanches. Nauka, Moscow, pp. 62–73. (in Russian)

Golubev, V.N., Ermakov, A.N., 1993. Some features of water vapor flow across the snow-soil interface. Materialy Gliaciol. Issled. 76, 19–24.

Golubev, V.N., Seliverstov, Yu.G., Sokratov, S.A., 1997. Flow of water vapor across the snow-frozen soil interface. Kriosfera Zemli I (3), 39–43.

Kutateladze, S.S., Borshanskiy, V.M., 1958. Heat Transfer. A Handbook. Gosenergoizdat, Moscow, Leningrad, 414 pp. (in Russian)

Liston, G.E., Sturm, M., 2004. The role of winter sublimation in the Arctic moisture budget. Nordic Hydrol. 35 (4–5), 325–334.

Mikheev, M.A., Mikheeva, I.M., 1977. Fundamentals of Heat Transfer. Second Edition. Energiya, Moscow, 344 pp. (in Russian)

Neumann, T.A., Albert, M.R., Engel, C., Courville, Z., Perron, F., 2009. Sublimation rate and the mass-transfer coefficient for snow sublimation. Intern. J. Heat Mass Trans. 52, 309–315.

Pavlov, A.V., 1975. Soil-Air Heat Exchange in Northern and Middle Latitudes of the USSR. Izd. AN SSSR, Yakutsk, 302 pp. (in Russian)

Strasser, U., Bernhardt, M., Weber, M., Liston, G.E., Mauser, W., 2008. Is snow sublimation important in the alpine water balance? Cryosphere 2, 53–66.

Sturm, M., Holmgren, J., Konig, M., Morris, K., 1997. The thermal conductivity of seasonal snow. J. Glaciol. 43 (143), 26–41.

Received July 1, 2014